

Comments on Advanced, Time-Resolved Imaging Techniques
for Free-Electron Laser (FEL) Experiments*

by

Alex H. Lumpkin

Advanced Photon Source
Argonne National Laboratory
9700 S. Cass Avenue - Bldg. 362
Argonne, Illinois 60439 USA
Telephone: (708)252-4879
FAX: (708)252-7187

DISCLAIMER

This report was prepared as an account of work sponsored by an agency of the United States Government. Neither the United States Government nor any agency thereof, nor any of their employees, makes any warranty, express or implied, or assumes any legal liability or responsibility for the accuracy, completeness, or usefulness of any information, apparatus, product, or process disclosed, or represents that its use would not infringe privately owned rights. Reference herein to any specific commercial product, process, or service by trade name, trademark, manufacturer, or otherwise does not necessarily constitute or imply its endorsement, recommendation, or favoring by the United States Government or any agency thereof. The views and opinions of authors expressed herein do not necessarily state or reflect those of the United States Government or any agency thereof.

*Work supported by the U.S. Department of Energy, Office of Basic Energy Sciences, under Contract No. W-31-109-ENG-38.

The submitted manuscript has been authored by a contractor of the U.S. Government under contract No. W-31-109-ENG-38. Accordingly, the U.S. Government retains a nonexclusive, royalty-free license to publish or reproduce the published form of this contribution, or allow others to do so, for U.S. Government purposes.

MASTER
DISTRIBUTION OF THIS DOCUMENT IS UNLIMITED

Comments on Advanced, Time-Resolved Imaging Techniques
for Free-Electron Laser (FEL) Experiments

Alex H. Lumpkin
Accelerator Systems Division
Advanced Photon Source
Argonne National Laboratory
Argonne, Illinois 60439 USA

Abstract

An extensive set of time-resolved imaging experiments has been performed on rf-linac driven free-electron lasers (FELs) over the past few years. These experiments have addressed both micropulse and macropulse timescales on both the charged-particle beam and the wiggler/undulator outputs (spontaneous emission and lasing). A brief review of first measurements on photoinjector micropulse elongation, submacropulse phase slew in drive lasers, submacropulse wavelength shifts in lasers, etc. is presented. This is followed by discussions of new measurements of 35-MeV electron beam micropulse bunch length (≤ 10 ps) using optical transition radiation, some of the first single bend synchrotron radiation beam profile measurements at $\gamma < 80$, and comments on the low-jitter synchroscan streak camera tuner. These techniques will be further developed on the 200-650 MeV linac test stand at the Advanced Photon Source (APS) in the next few years. Such techniques should be adaptable to many of the present FEL designs and to some aspects of the next generation of light sources.

1. Introduction

As free-electron laser (FEL) designs and speculation push to shorter wavelength and concomitant demands on accelerator performance (i.e., electron/positron beam quality), it is appropriate to comment on advanced, time-resolved imaging techniques that have been performed over the past few years and this year [1-3]. These experiments have addressed both micropulse and macropulse timescales on both the charged-particle beam and the wiggler/undulator outputs (spontaneous emission radiation (SER) and lasing). The experiments have relied on converting charged-particle parameter information to optical radiation via Cherenkov radiation (CR), optical transition radiation (OTR), synchrotron radiation (SR), SER, and FEL. Then, advanced, imaging techniques based on gated, intensified cameras and synchroscan as dual-sweep streak cameras can be used to detect the photons.

Besides the review of first measurements on longitudinal wakefields, first measurements of photoinjector micropulse elongation, submacropulse phase slew, submicropulse laser effects, and submacropulse wavelength shifts in FELs, etc., new demonstrations are discussed. These include results on 35-MeV electron beam micropulse bunch length (<10 ps) measurements using OTR, nonintercepting beam profile measurements using SR at $\gamma < 80$, and a new synchroscan tuning module with improved jitter and resolution. The OTR measurements and the new tuning module results are combined to address bunch length effects due to charge and/or transverse wakefield effects. These concepts of diagnosis of FEL time-dependent aspects can be used to improve delivered performance to the user community as well.

2. Imaging Background and Examples

The imaging techniques have the basic components of source, conversion mechanism, detection, and data acquisition/analysis. Once the beam information is carried in the photon field of appropriate wavelength for the detector (110 to 800 nm:S20 photocathode, 300 to 1300 nm:S1 photocathode), the gated, intensified cameras and streak cameras can be used. The image position may correspond to spatial position, energy, or phase, while the image profile may be spatial profile, energy spread, or bunch length depending on the experimental setup.

Some examples of critical time-resolved imaging results are mentioned below. Most of these impacted transform-limited FEL bandwidth until the causes were addressed and the effects reduced.

- a) Observation of longitudinal wakefields in the Los Alamos wiggler [4].
- b) Micropulse bunch length change during the macropulse (Boeing visible FEL) [5].
- c) Wavelength shift within a micropulse (Boeing visible FEL) [3].
- d) FEL wavelength slew during a macropulse [6].
- e) Drive laser phase slew during a macropulse [7].

Additionally, to improve our capabilities, a higher-Q tuner was obtained for our Hamamatsu synchroscan streak camera. The drive laser stability was evaluated by a demo Hi-Q tuner, our new high-Q tuner, and the standard M1954 tuner as shown in Table I. The jitter in the laser plus the camera of ~ 1 ps (rms) was obtained by assuming that the camera resolution and jitter, the laser bunch length, and the laser jitter could be treated in quadrature.

Since the jitter value is small compared to the bunch lengths of 8-10 ps, the absolute error for this test is difficult to specify. However, the relative performance is seen to be in good agreement. On the basis of this comparison, the new streak tuner and synchroscan streak camera were installed in the accelerator vault for electron beam characterization described in the next section.

3. New Results and Future Prospects

Recent results from the ongoing diagnostics development effort at Los Alamos include optical transition radiation, synchrotron radiation, and synchroscan (high-Q) streak camera aspects.

For reference, the beamline is shown in Fig. 1. The measurements are concentrated in the region after the fourth accelerator with screen #4 plus the zero-degree port and 15° port in the 30°-bend vacuum chamber. The first port is used to look down the bore of the accelerator beamline to image the back interface of the interferometer via OTR's forward radiation. The second port is used to access SR emitted near the center of the 30° bend. The diagnostics assembled around this region are shown in Fig. 2. In particular, the streak camera viewed the OTR foil and the intensified charge-injection device (ICID) camera viewed the SR source in these initial experiments for the following discussion.

In Fig. 3, the use of OTR as a bunch length diagnostic in the on-axis, center image is straightforward with synchroscan techniques that synchronously summed 10's of pulses. As can be seen however, off-axis steering of the beam through tanks 3 and 4 results in transverse spatial kicks (head-to-tail) during the micropulse. As noted elsewhere [8-10], this diagnostic

can then be used to guide the on-line compensation of wakefields in the accelerators by steering in the fourth tank until the x-projection is minimized.

Another new result which has been reported by M.D. Wilke et al. [8], involves the further demonstration of using synchrotron radiation to image noninterceptively the beam spot in the 30° bend. To our knowledge no other FEL group (perhaps even linac group) has worked at $\gamma < 80$ and obtained on-line results. In our intensifier, the S20 photo cathode with quartz window has Q.E. from ~ 200 nm to 800 nm. At 40 MeV and for a 30 cm bend, the critical wavelength, λ_c , is 2 to 3 μm , but this leaves 1/2 the power at shorter wavelengths although in a narrow spectral regime. We estimated this four years ago and then at last year's conference, Greeger and Lumpkin [11] reported more of the scaling calculations. The MCP gain was actually turned to minimum for the 40-MeV, 20- μs long macropulse, with 1 to 2 nC per micropulse. Since the critical wavelength goes inversely with γ^3 , the signal drop off from 40 to 25 MeV is the combination of the γ^4 power term and the spectral shift (which dominates). In Fig. 4, the observed signal was normalized to charge, but no adjustment for the S20 PC spectral sensitivity has been made. Since we use synchroscan streak techniques, any imageable beam can also have its bunch length determined. The 25-40 MeV regime should be of interest to several FEL labs since they operate in the 20-65 MeV regime (see conference proceedings). This appears to be an untapped technology for FELs. Just before the conference, I used the relative other end of the SR spectrum (still visible photons) from a 3-GeV beam in a 12.8 m bend radius at SPEAR. We imaged a single bunch from one pass in this bending magnet.

Trends towards shorter wavelength, higher beam energies, and/or microwigglers continue to make these techniques relevant. Effects during the microwiggler current pulse over the macropulse could be assessed by time-resolved spectrometer work, for example. *The applicability down to the 110 to 200 nm region is direct, but an adjustment is needed in the vacuum ultraviolet (VUV). Once the vacuum interface is made though, XUV and soft x-rays are accessible from the instrumentation point of view.*

The Fourth Generation Light Source Workshop [12] identified a number of key beam parameters for linac-driven sources. Several of these are shown in Table II and are close to those expected for the Advanced Photon Source (APS) undulator test line [13]. Adaptation of diagnostic techniques for this regime at APS should provide interesting information to the FEL community interested in self-amplified spontaneous emission (SASE) in the next few years.

4. Summary

In summary, time-resolved diagnostics are critical to the optimization of both accelerator and FEL performance. These activities support the user demands for a stable FEL. At this 1992 FEL conference, it is noted that several of the user laboratories have developed their own versions of time-resolved techniques with image dissector tubes, fast readout of linear arrays, etc. The interaction of experimentalists and theorists needs to be as convolved as that of the electrons (positrons) with the electromagnetic fields in the FEL to determine the best way to reduce time-dependent effects. Finally, because of the nature of these imaging techniques, they should be adaptable to many of the planned FELs and to some aspects of the next generation of light sources where low emittance, higher energy beams, short wavelengths, microwigglers, etc. will be involved.

Acknowledgments

The author acknowledges the Los Alamos FEL diagnostics team, particularly Mark Wilke, Scott Appar, Renee Feldman, and Clint Webb for their efforts and the operations team including Don Feldman, Jim Early, and Pat O'Shea for past and more recent beam time. He also acknowledges the simulations section at Los Alamos including John Goldstein, Mark Schmitt, Bruce Carlsten, Brian McVey, Bob Tokar, and Les Thode for their calculations and suggestions over the past few years.

References

- [1] Alex H. Lumpkin, NIM A296 (1990) 134.
- [2] Alex H. Lumpkin, NIM A318 (1992) 442.
- [3] A.H. Lumpkin, S.P. King, M.D. Wilke, S.P. Wei and K.J. Davis, NIM A285 (1989) 17.
- [4] A.H. Lumpkin, D.W. Feldman, R.W. Warren, W.E. Stern and K.C.D. Chan, Nucl. Inst. and Meth. in Phys. Res. A296 (1990) 186.
- [5] Alex H. Lumpkin, NIM A318 (1992) 442.
- [6] A.H. Lumpkin, et al., NIM A296 (1990) 169.
- [7] Alex H. Lumpkin and James W. Early, NIM A318 (1992) 389.
- [8] M.D. Wilke, A.H. Lumpkin, P.G. O'Shea E.J. Pitcher and R.B. Feldman, "Electron-Beam Diagnostics Development for the Los Alamos FEL Facility," Proceedings of International Linac Conference, Ottawa, Canada, August 25-28, 1992.
- [9] Alex H. Lumpkin and Mark D. Wilke, "Time-Resolved Electron-Beam Characterizations with Optical Transition Radiation," Proceedings of the Fourteenth International Free-Electron Laser Conference, Kobe, Japan, August 24-28, 1992.
- [10] P.G.O'Shea, et al., "Performance of the APEX Free-Electron Laser at Los Alamos National Laboratory," these Proceedings (1992).
- [11] R.B. Greigor and A.H. Lumpkin, NIM A318 (1992) 422.
- [12] M. Cornacchia and H. Winick (ed), "Workshop on Fourth Generation Light Sources," February 24-27, 1992, SSRL 92/02.
- [13] M. Borland (Argonne National Laboratory), private communication, June 1992.

**Table I Evaluation of Drive Laser Phase with Three Tuner Modules
(Data of 12/3/91)**

Tuner Module	Calibration Factor (ps/ch)	Total Observed Bunch Length, 1 macropulse (ch)	Bunch Length (ps) ⁺	Total Observed Bunch Length, 20	Estimated Jitter (PS)	
					FWHM	RMS
Demo, Hi-Q	0.85	13.37	10.6	13.69	2.48	1.06
New Hi-Q	0.75	14.41	10.3	14.83	2.6	1.12
Standard Tuner (M1954)	1.25	8.92	9.3	9.12	2.37	1.01

o All entries, at least 5 sample averages

o 20- μ s macropulse in green component

+ Autocorrelator-measured fundamental bunch length: 9.8 ps (FWHM)

TABLE II Beam parameters for the undulator test line at APS as compared to 4th Generation Workshop values (ref. 12)

<u>Parameter</u>	<u>APS</u>	<u>4th Generation Workshop (Linac)</u>
Emittance (Π mm mrad) (rms, normalized)	2	1.5
Peak Current (kA)	1/2 to 1	1
Bunch Length (ps)	<1 to 15	~1
Energy (MeV)	200-650	100-1000
Energy Spread	0.1 %	0.05 %
Macropulse Bunch Length	30 ns	--

Figure Captions

- Fig. 1** Schematic of the Los Alamos FEL beamline. The accelerator, wigglers, and some diagnostics locations are indicated.
- Fig. 2** Schematic of an expanded view of the diagnostics assembled around the first 30° bend in the beam transport. The streak camera views the back surface of screen 4 and one ICID views the SR source at a 15° port.
- Fig. 3** Composite synchroscan streak images of the beam x-profile and bunch length at station 4. The OTR conversion mechanism is used to generate the visible image.
- Fig. 4** Dependence of observed SR signal in the intensified, charge-injection device (ICID) camera on the electron beam gamma (energy).

APEX ELECTRON BEAM DIAGNOSTICS

KEY

CS	SIT CAMERA	S	OTR SCREEN
CI	INT. CID	M	MAGNETIC SPECTROMETER
CV	VIDICON	Q	QUAD
CIV	INT. VIDICON	CIH	HALO CI
W	WALL CURRENT MON.	CIS	SYNCHROTRON CI

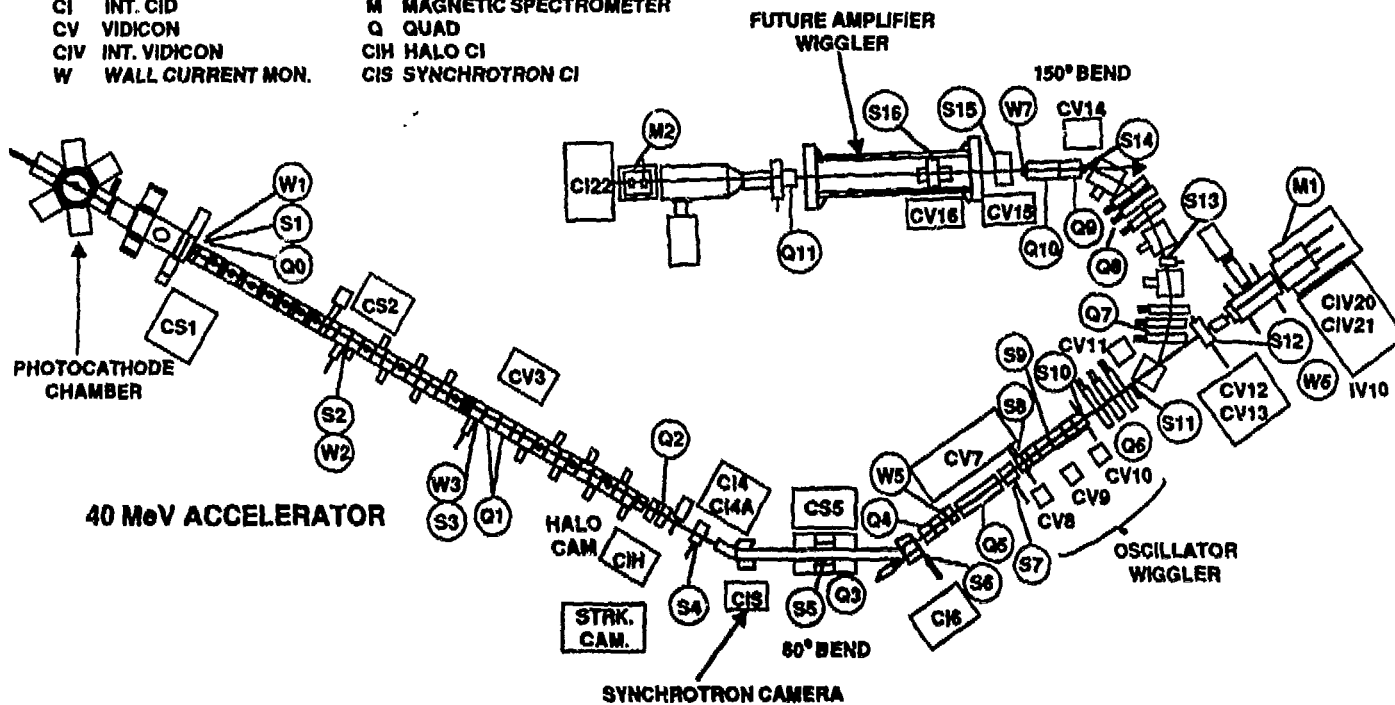


Fig. 1

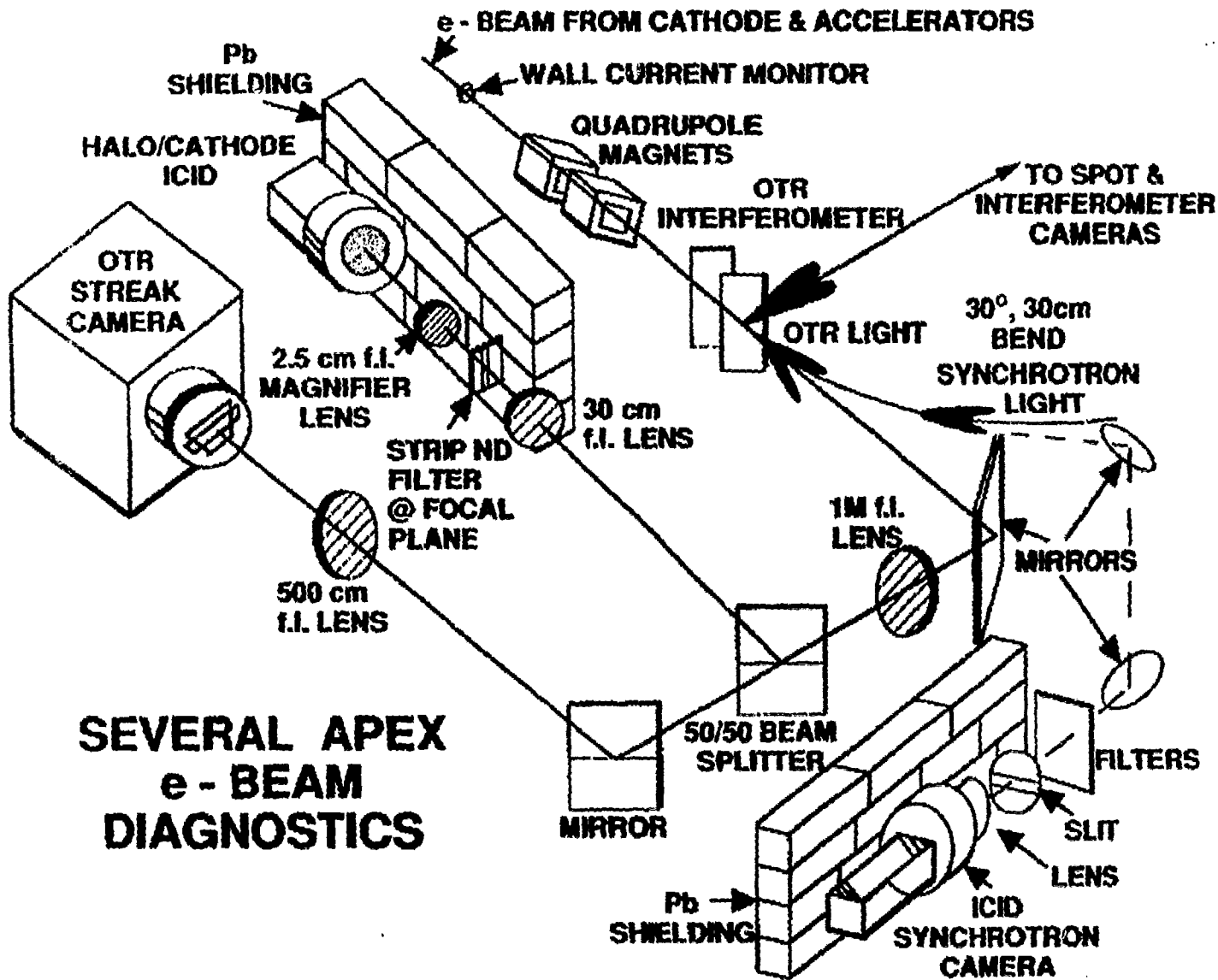


Fig. 2

WAKE FIELD OBSERVATIONS AT SCREEN 4

$E = 41 \text{ MeV}$

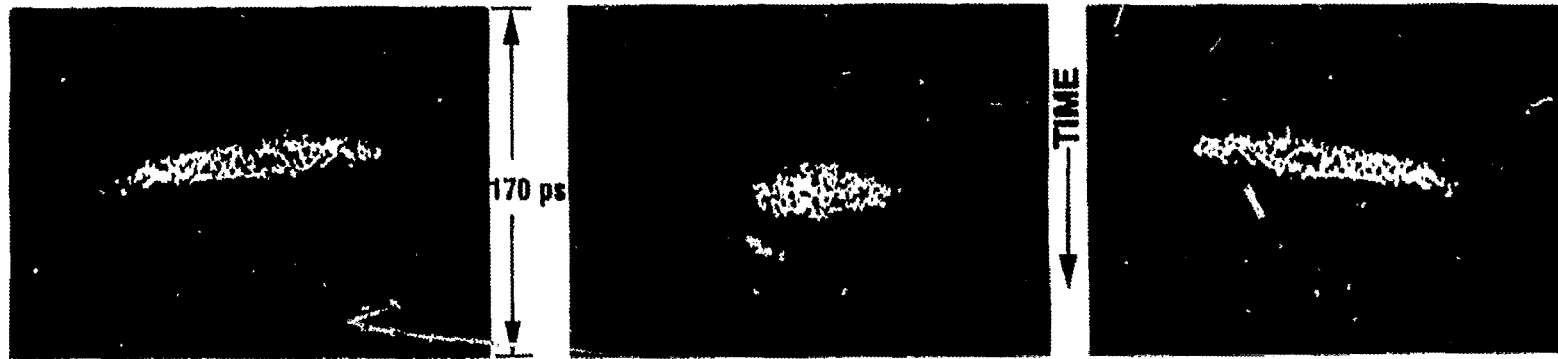
$q_{\mu} = 4 \text{ nC}$

$\tau_M = 20 \mu\text{sec}$

$\tau_{\mu} = 17.5 \text{ ps}$

$\tau_{\mu} = 14.5 \text{ ps}$

$\tau_{\mu} = 12.5 \text{ ps}$



a) 5.5 mm Left on screen 3

b) Centered on screen 3

c) 3.5 mm Right on screen 3

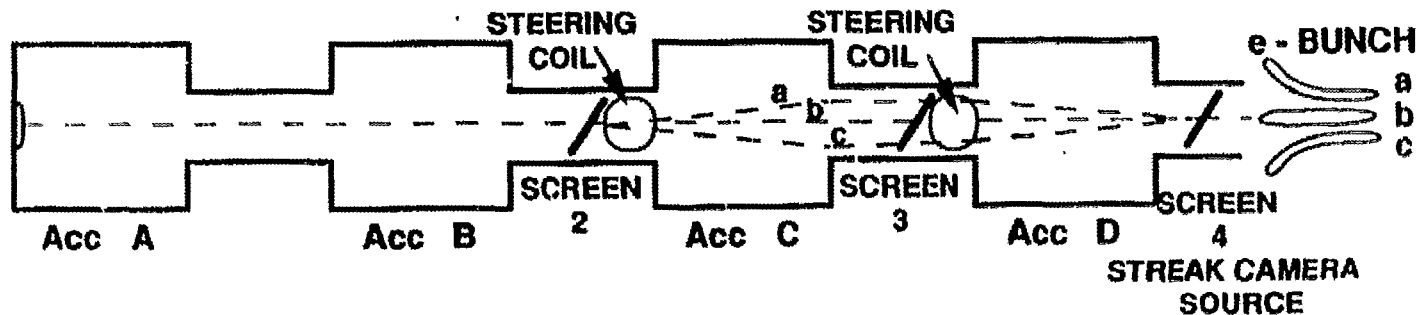


Fig. 3

SYNCHROTRON SIGNAL vs BEAM ENERGY FOR 30 cm BEND

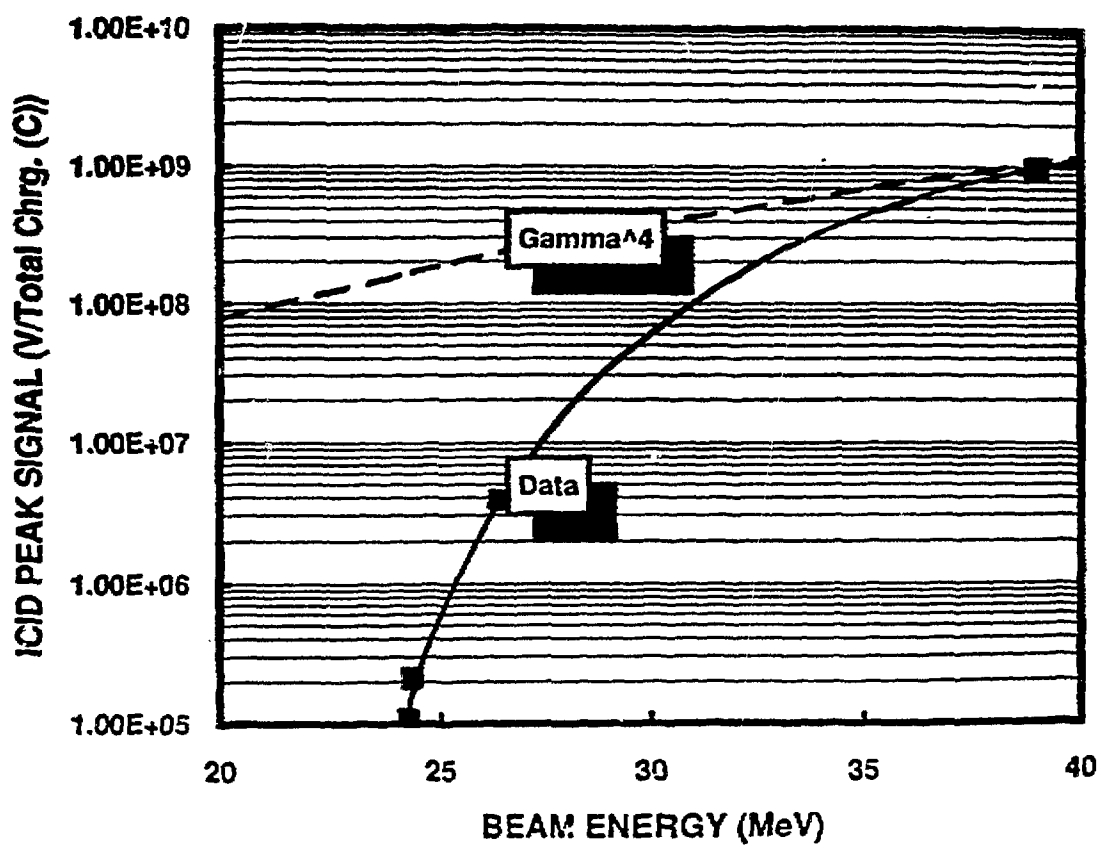


Fig. 4

**REVIEW OF ADVANCED, TIME-RESOLVED IMAGING TECHNIQUES
FOR FREE-ELECTRON LASER EXPERIMENTS**

**ALEX H. LUMPKIN
ADVANCED PHOTON SOURCE
ARGONNE NATIONAL LABORATORY**

The submitted manuscript has been authored
by a contractor of the U. S. Government
under contract No. W-31-109-ENG-38.
Accordingly, the U. S. Government retains a
nonexclusive, royalty-free license to publish
or reproduce the published form of this
contribution, or allow others to do so, for
U. S. Government purposes.

NOV 12 1992

ADVANCED PHOTON SOURCE

Imaging Techniques Will Have A Number of Diagnostic Applications

- Charged-particle beam parameters can be accessed by intercepting and nonintercepting radiation conversion techniques.

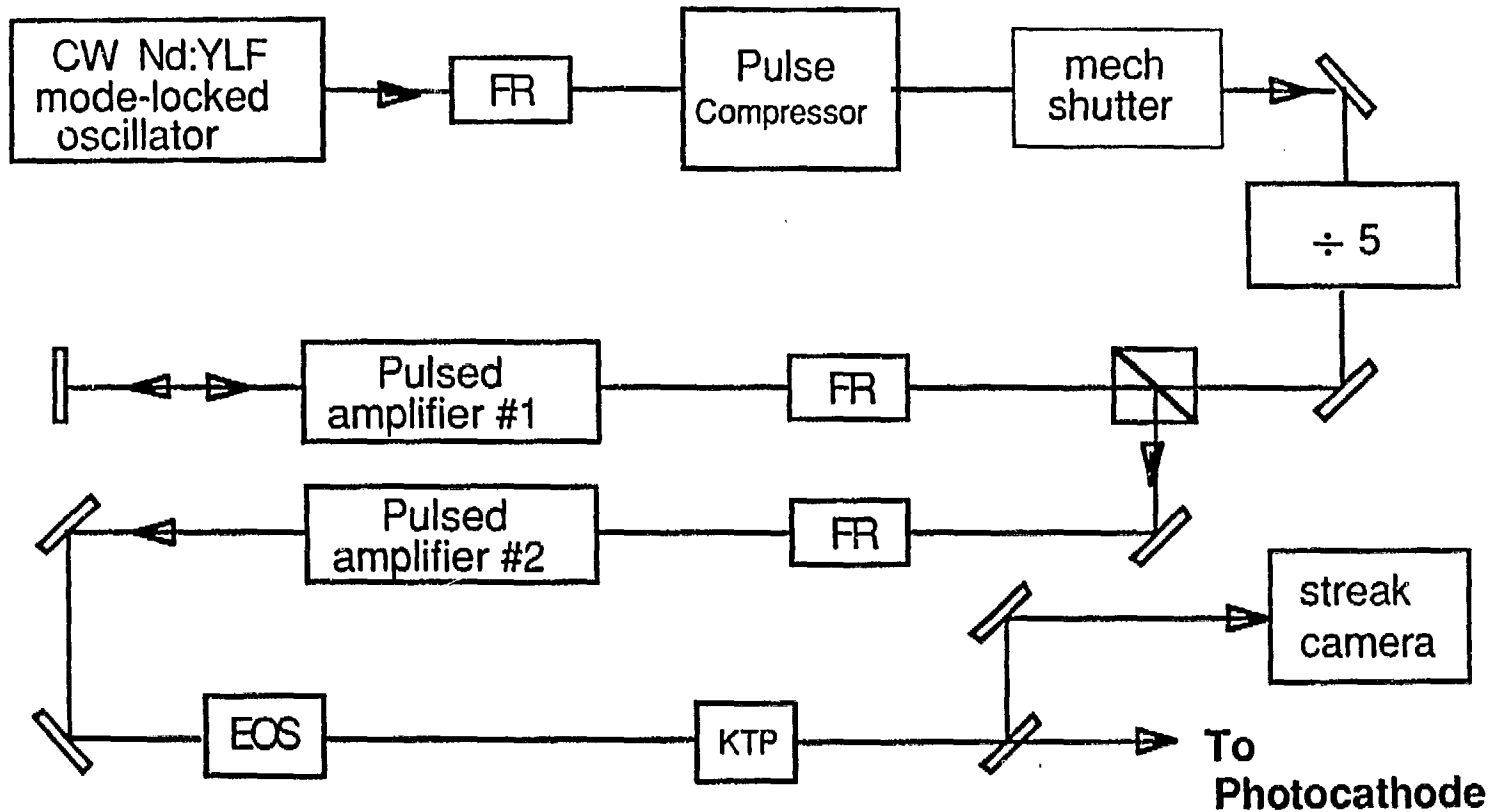
Intercepting: Fluorescence (FL)
 Optical Transition Radiation (OTR)
 Cherenkov Radiation (CR)

Nonintercepting: Synchrotron Radiation (SR)
 Undulator Radiation (UR)

- Conversion to photons allows visible, ultraviolet, or x-ray imaging techniques to be used.
- Data acquisition through video digitizing and image analysis.

Position: Spatial
 Energy
 Time (phase)

Profile: Size
 Energy Spread
 Bunch Length



FR = Faraday rotator optical isolator

EOS = Electro-optic shutter

KTP = Potassium titanyl phosphate frequency doubling crystal

÷ 5 = Fast pockels cell shutter transmitting every fifth pulse

DUAL-SWEEP STREAK CAMERA TRACKS DRIVE-LASER PHASE EFFECTS (Cavity and Stabilizer)

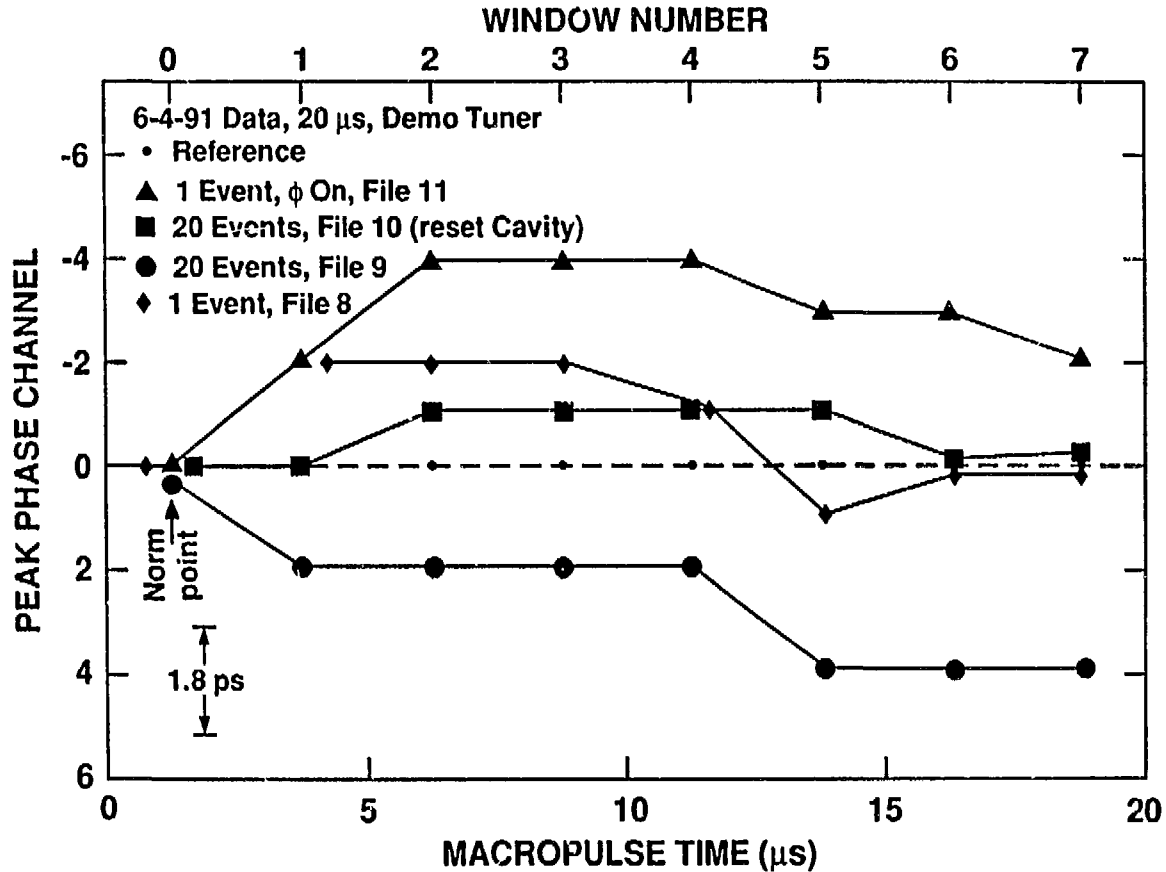


Table IV. Unexpected Micropulse Length for Drive Laser Fundamental Identified with Streak Camera

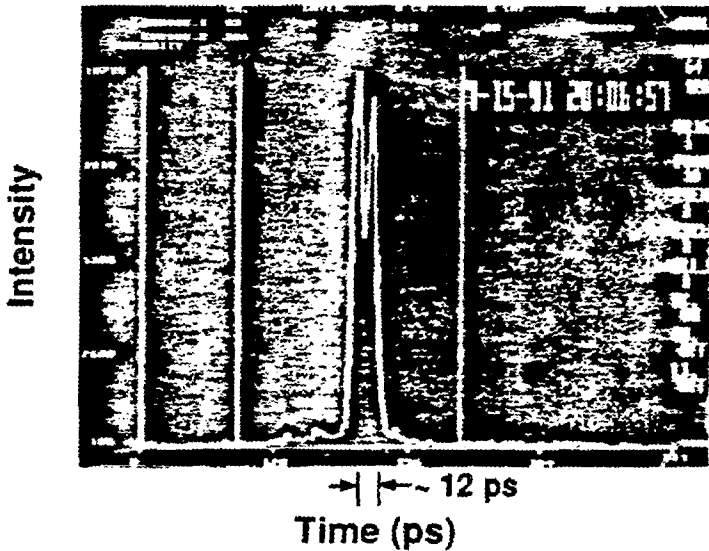
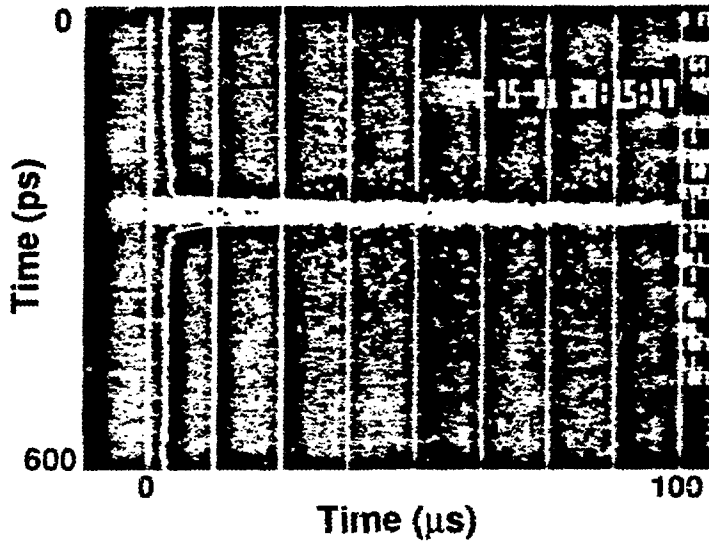
Data Date	Pulse Compressed Micropulse (FWHM ps)*	Oscillator Output		Fast** Photodiode (FWHM ps)
		Streak Range/AC	FWHM (ps)	
4-12-91	6.7	1	30	60
4-12-91	6.7	2	31	60
4-12-91	16.5	2	42	71
4-12-91	16.5	1	42	71
4-15, 16-91	6.7	AC	30	--
	16.5	AC	42	--

Note: Generally stated that oscillator micropulse length is 50 - 60 ps.

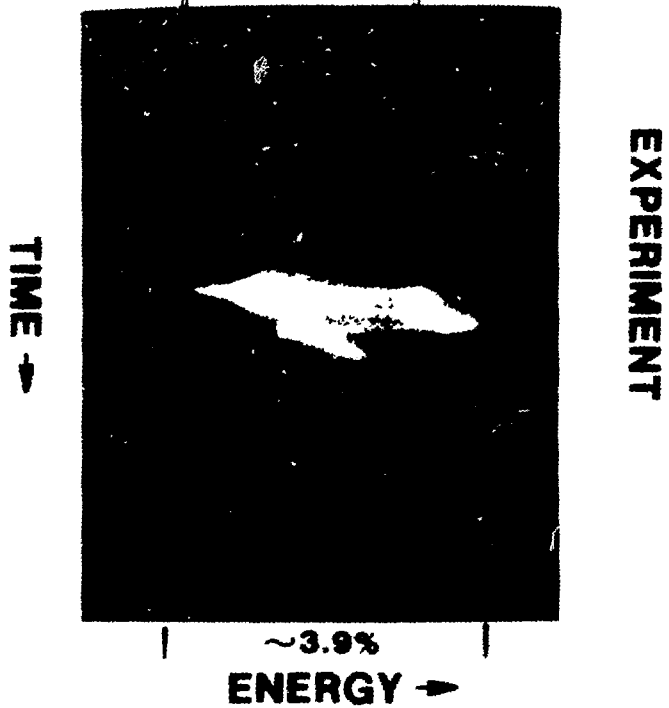
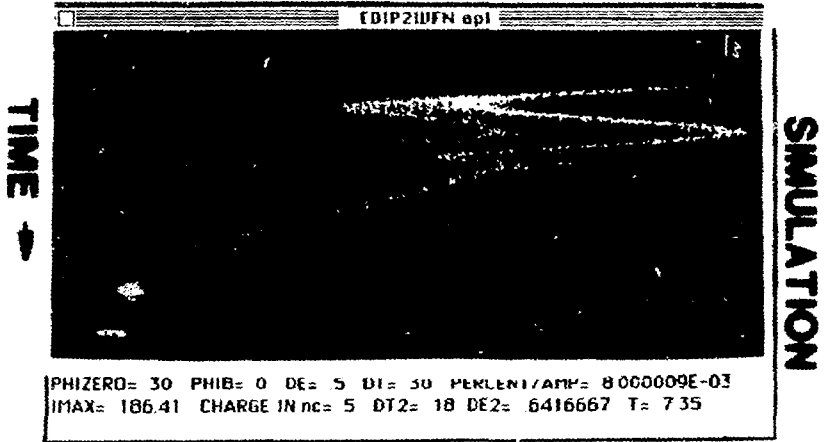
* Autocorrelator (AC) measurement on infrared

** "fast" photodiode limiting resolution about 45 ps in quadrature with laser micropulse

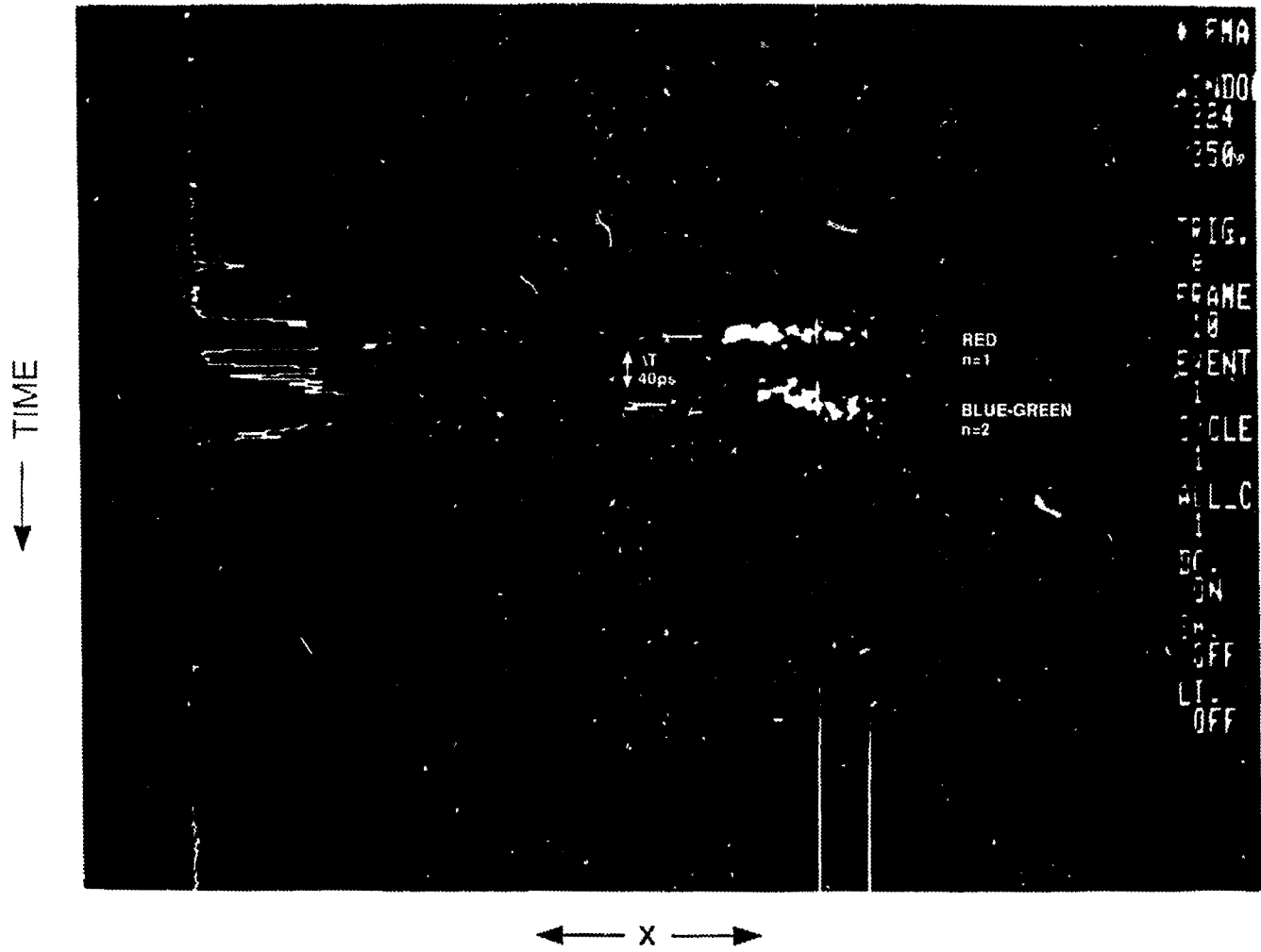
DUAL-SWEEP TECHNIQUE USED TO DISPLAY SUBMACROPULSE EFFECTS (8-29-90)



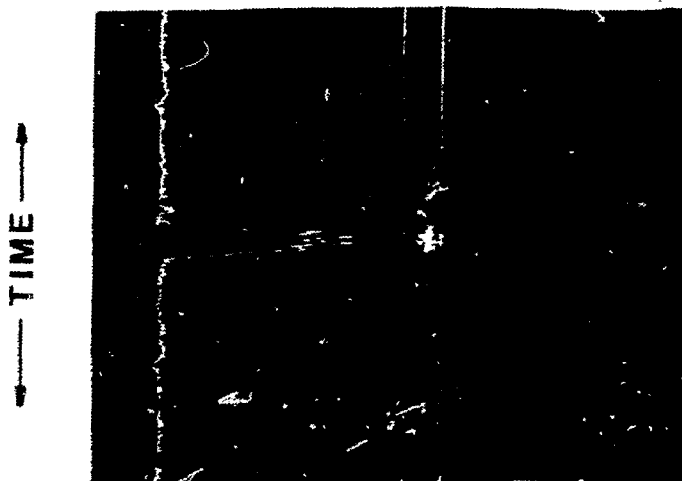
ENERGY



STREAK IMAGE ON MICROPULSE SHOWS TWO STRUCTURES, FUNDAMENTAL PLUS SECOND HARMONIC

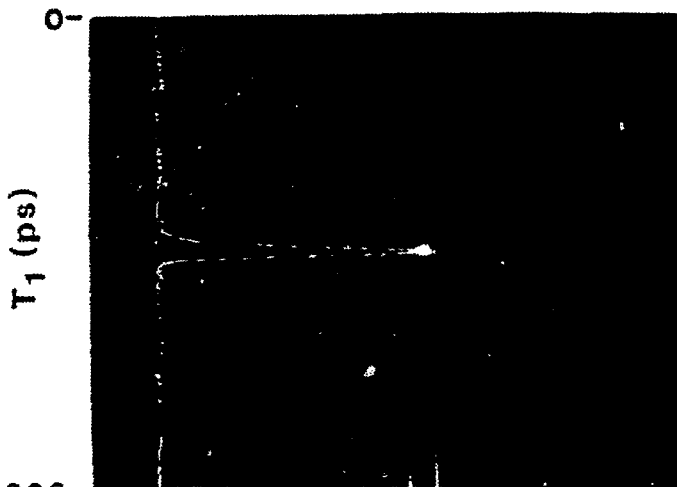


SYNCHROSCAN STREAK PROVIDES
BUNCHING DIAGNOSTIC FROM
OUTCOUPLED SPONTANEOUS RADIATION
(MACROPULSE)



FWHM
=27.8ps

← X →

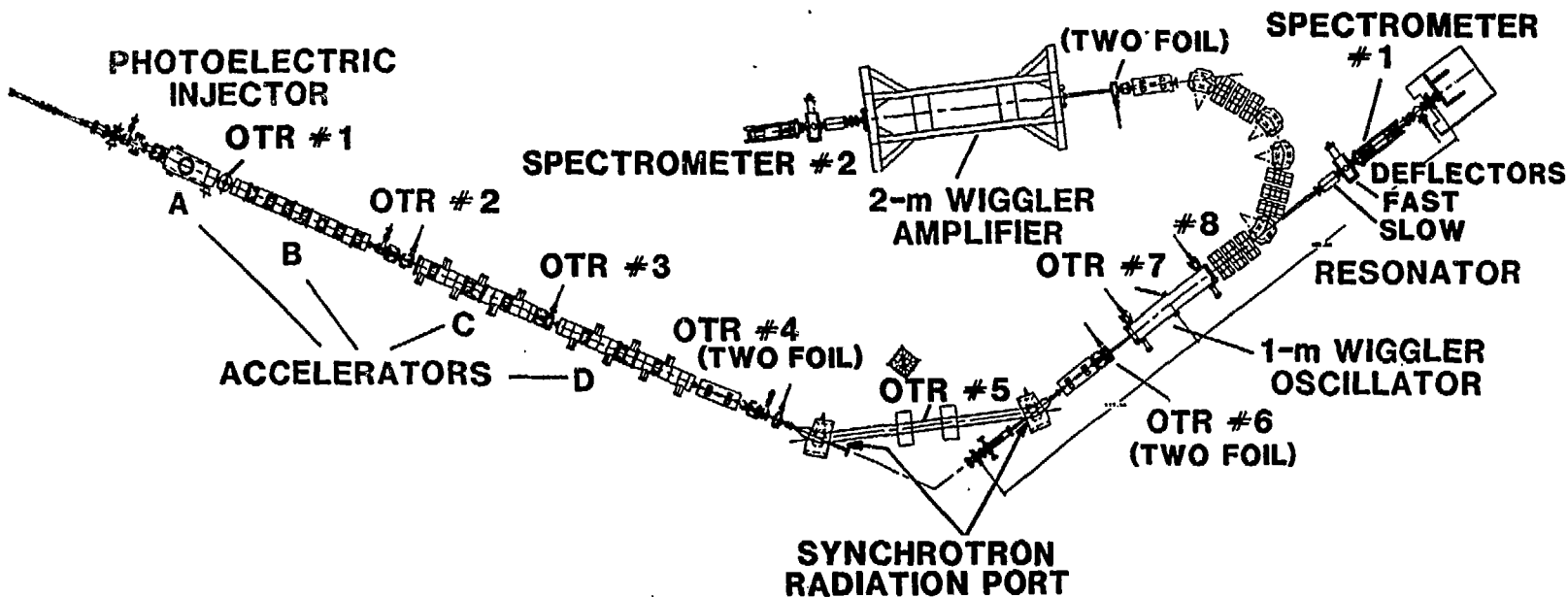


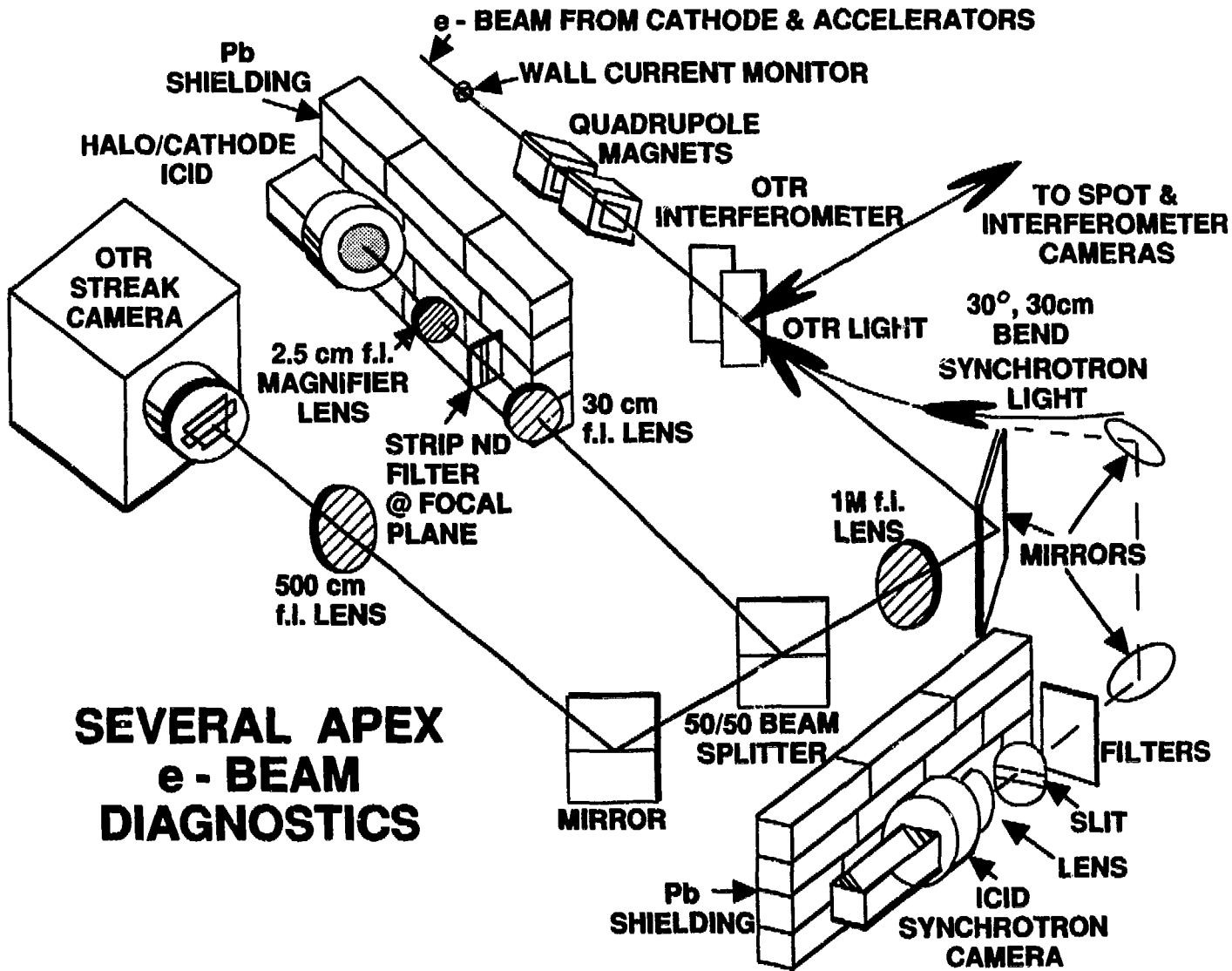
FWHM
=12ps

108MHz SHB(1)
433MHz SHB(1/3)

← X →

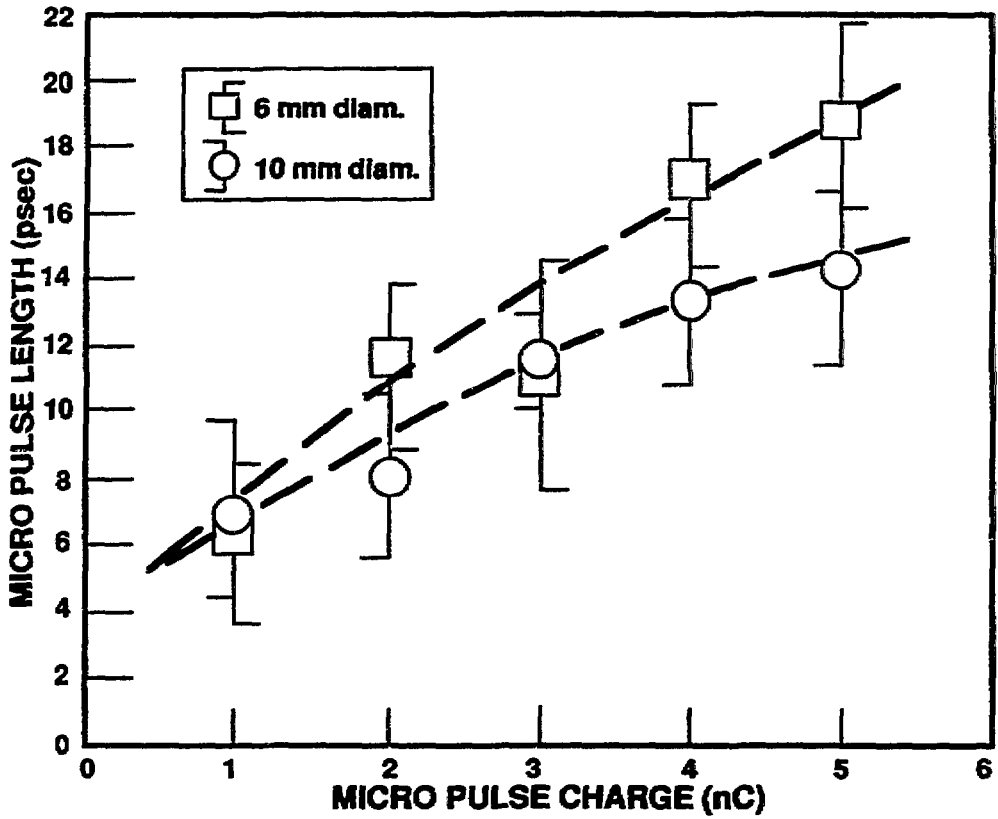
Schematic of APEX Master Oscillator Power Amplifier (MOPA)





**SEVERAL APEX
e - BEAM
DIAGNOSTICS**

MICRO PULSE LENGTH



WAKE FIELD OBSERVATIONS AT SCREEN 4

$E = 41 \text{ MeV}$

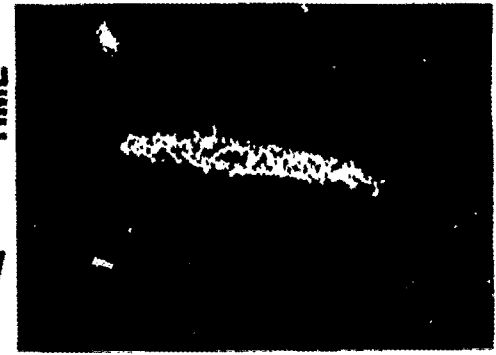
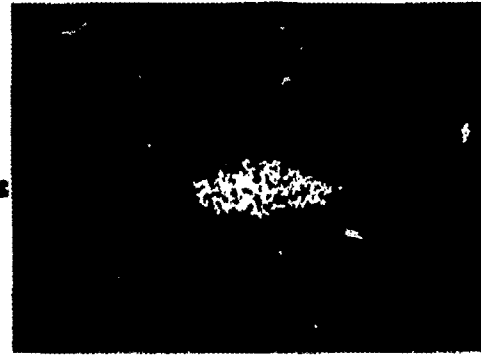
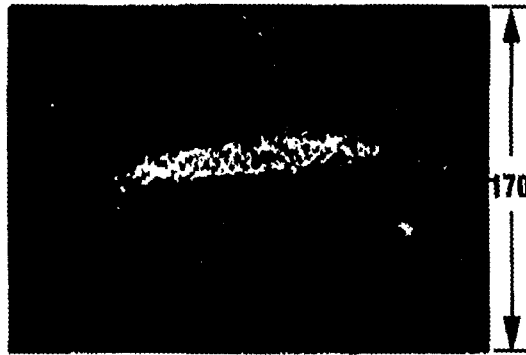
$q_{\mu} = 4 \text{ nC}$

$\tau_M = 20 \mu\text{sec}$

$\tau_{\mu} = 17.5 \text{ ps}$

$\tau_{\mu} = 14.5 \text{ ps}$

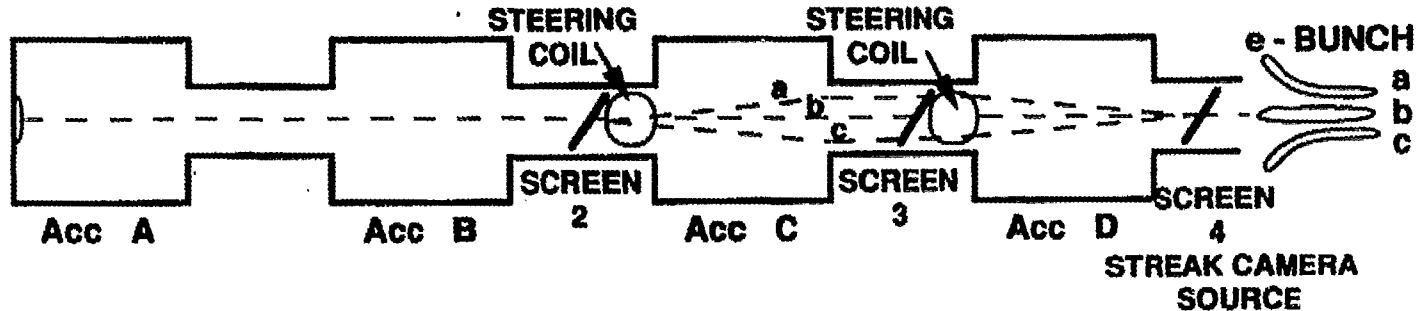
$\tau_{\mu} = 12.5 \text{ ps}$



a) 5.5 mm Left on screen 3

b) Centered on screen 3

c) 3.5 mm Right on screen 3



SUMMARY

In summary, we have performed a series of synchroscan and dual-sweep streak measurements on a PEI drive laser and on the e-beam from a thermionic/subharmonic buncher system. Effects on the micropulse time scale during the macropulse have been identified in both cases. Adjustments to the systems resulted in improved performance as guided by these measurements.